Diiron(III) oxo-bridged complexes with BPMEN and additional monodentate or bidentate ligands: Synthesis and reactivity in olefin epoxidation with H_2O_2[☆]

Sonia Taktak, Sergey V. Kryatov, Terry E. Haas, Elena V. Rybak-Akimova[*]

Department of Chemistry, Tufts University, Medford, MA 02155, USA

S.K. and E.R.A. would like to dedicate this paper to their mentor, Vitaly V. Pavlishchuk, on the occasion of his 50th birthday.

Abstract

The reactivity of a series of diiron(III) complexes (**1–5**) of the tetradentate ligand bpmen (*N,N'*-dimethyl-*N,N'*-bis(2-pyridylmethyl)ethane-1,2-diamine) has been investigated. Three new diiron(III) complexes (**3–5**) with fluoride and acetate ligands have been isolated and structurally characterized. Complex $Fe_2(III)(\mu\text{-O})(\mu\text{-OH})(bpmen)_2$ (**1**), which contains a μ-oxo, μ-hydroxo diiron(III) diamond core, was found to catalyze the epoxidation of cyclooctene with hydrogen peroxide, but its μ-oxo, μ-acetate counterpart $Fe_2(III)(\mu\text{-O})(\mu\text{-OAc})(bpmen)_2$ (**2**) is unreactive. The effect of additives such as hydrofluoric acid, tetrabutylammonium fluoride, acetic acid and acetate on the reactivity of **1** and **2** is reported. Complexes **3–5** with two monodentate ligands (F^- or OAc^-) attached to the bpmen-supported μ-oxo bridged diiron(III) core do not activate H_2O_2 for olefin epoxidation.
© 2006 Elsevier B.V. All rights reserved.

Keywords: Epoxidation; Iron complexes; Hydrogen peroxide

1. Introduction

Oxo-bridged diiron complexes with neutral tetradentate aminopyridine ligands [1–3] are an important class of structural and functional models of diiron non-heme metalloenzymes like methane monooxygenase, ribonucleotide reductase or purple acid phosphatase [4–7]. A relatively simple ligand bpmen (where bpmen = *N,N'*-dimethyl-*N,N'*-bis(2-pyridylmethyl)ethane-1,2-diamine) was successfully used to prepare both mononuclear [8–10] and dinuclear iron complexes [10–15], some of which were shown to activate small molecules (e.g., H_2O_2) and catalyze oxidation reactions. In particular, $[Fe^{II}(bpmen)(CH_3CN)_2](ClO_4)_2$ is a well known catalyst in alkene epoxidation with hydrogen peroxide [16–18]. Its catalytic activity was reported to be enhanced by the presence of acetic

acid and some counterions (e.g., SbF_6^-), but the nature of the active species remains unclear [17,19].

Hydrogen peroxide is capable of oxidizing iron(II) into iron(III) in its complexes with bpmen, especially in the presence of additional carboxylate ligands [20]. The initially formed mononuclear iron(III) complex may undergo further reactions with various components of epoxidizing solutions, producing an active oxidant [21,22]. It would be advantageous to use air-stable iron(III) complexes instead of their air-sensitive iron(II) precursors in oxidation catalysis. However, mononuclear iron(III) complexes with tetradentate aminopyridine ligands are unstable in the absence of additional pre-coordinated ligands and easily form oxo-bridged dimers [1,17,23–25]. While an oxo-bridged diiron(III) complex with a dinucleating, covalently linked aminopyridine ligand was recently reported to catalyze olefin epoxidation with H_2O_2 [26], the reactivity of diiron(III) complexes supported by simple, easy to synthesize mononucleating ligands (e.g., bpmen) is not completely understood.

One of the best-characterized diiron(III)-bpmen complexes is an μ-oxo-, μ-hydroxo diiron(III) complex **1**, which undergoes ring-opening upon reaction with water [10,14,27], and

---
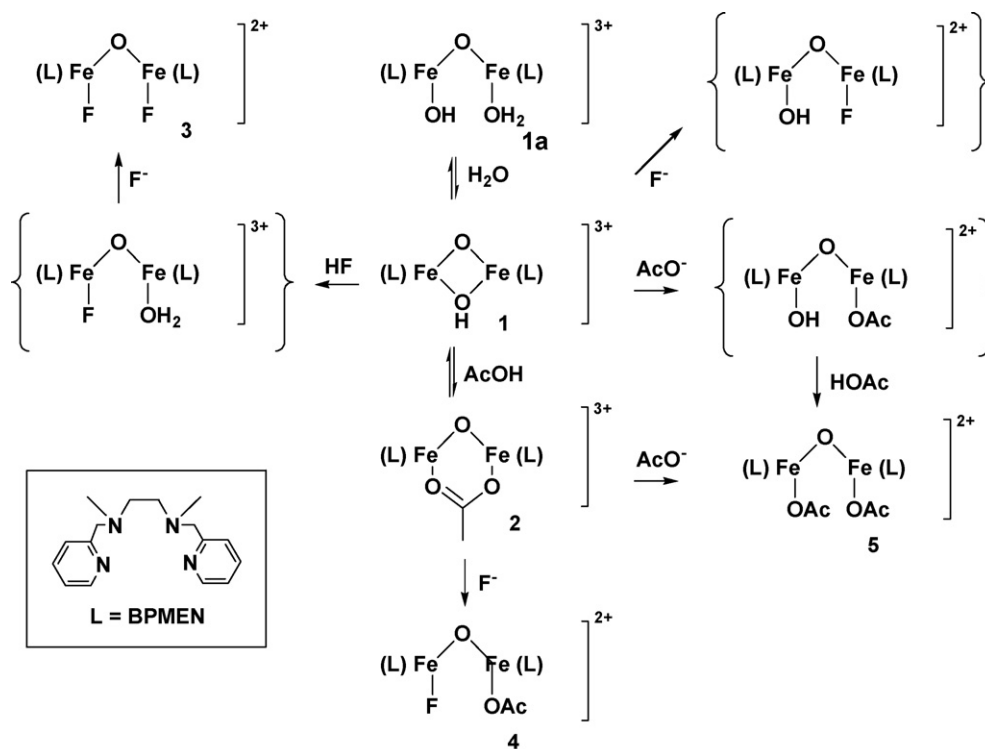
Scheme 1. Series of reactions studied in this work and numbering of some of the species involved.

reacts with acetic acid producing a dinuclear μ-oxo, μ-acetate diiron(III) complex **2** (Scheme 1) [12]. It was proposed that dinuclear μ-oxo, μ-acetate diiron(III) complex **2**, formed in situ under olefin epoxidation conditions, is the catalytically active species [17]. However, contradictory observations have been later reported on the reactivity of independently prepared complex **2** [18,28], possibly due to different reaction conditions used.

In order to better understand the role of iron coordination environment in the catalytic activity of diiron(III) complexes and the effect of additives and counterions on alkene epoxidation reactions, we investigated the reactivity of dinuclear iron(III) bpmen complexes **1** and **2** with fluoride and acetate ligands and their protonated forms (hydrofluoric acid and acetic acid). One or two acetate ions can, in principle, coordinate to **1** in either monodentate or bidentate mode, and this coordination may account for epoxidation enhancement in the presence of acetic acid (Scheme 1). Our selection of fluoride as a monodentate ligand was guided by reports on positive effects on epoxidation yields exerted by SbF_6^- counterions [17], which may generate F^- upon partial hydrolysis. The products of mono- or bidentate ligand addition to **1** and **2** were identified by UV–vis, ESI-MS and in some cases by single-crystal X-ray diffraction. The effect of additives and the role of protons in olefin epoxidation were monitored by running comparative catalysis experiments.

2. Experimental

2.1. General

All reagents were obtained from commercially available sources and used without further purification, unless otherwise noted. Tetraethylammonium acetate was generated in solution by mixing equimolar amounts of acetic acid and tetraethylammonium hydroxide in acetonitrile. The ligand bpmen was synthesized according to a published procedure [14]. Complexes **1** [10] and **2** [12] were prepared as described elsewhere. UV–vis spectra were acquired on a Hitachi U-2000 or on a JASCO V-570 spectrophotometer. Gas chromatography (GC) analyses were performed on a Hewlett-Packard 5890 GC instrument equipped with an FID detector and HP Chemstation 6.01 software. Electrospray mass spectra were recorded on a Finigan LTQ mass spectrometer in the positive ion detection mode. Elemental analyses were performed by QTI (Whitehouse, NJ). Reactions involving HF were performed in plastic vials. CAUTION: Although no problems were encountered in this study, perchlorate salts of metal complexes with organic ligands are potentially explosive and should be handled with care!

2.2. Isolation of solid complexes.

2.2.1. $[Fe_2(\mu\text{-}O)(bpmen)_2F_2](ClO_4)_2 \cdot 2CH_3CN$ (**3**)

Ligand bpmen (0.63 g, 2.33 mmol) was dissolved in 10 mL of ethanol containing triethylamine (455 μL, 3.26 mmol) and slowly added to a solution of $Fe(ClO_4)_3 \cdot 6H_2O$ (1.19 g, 2.32 mmol) in 5 mL ethanol. Tetrabutylammonium fluoride, 75% in water (0.58 g, 2.22 mmol), dissolved in 5 mL ethanol, was added to the previous mixture. The reaction was allowed to proceed overnight, and an orange/brown precipitate formed. After filtration, the solid was dissolved in 100 mL of warm acetonitrile and left in the freezer. An orange powder precipitated overnight. Yield of crude orange material: 221 mg

(20%). Orange crystals suitable for X-ray diffraction were obtained by vapor diffusion of diethyl ether in acetonitrile. Yield after crystallization: 100 mg (9%). ES-MS(+) (CH$_3$CN): *m/z* 805 ({[Fe$_2$(μ-O)(bpmen)$_2$F$_2$](ClO$_4$)}$^+$, 56), 353 ({[Fe$_2$(μ-O)(bpmen)$_2$F$_2$]}$^{2+}$, 100). Anal. Calcd. (found) for C$_{34}$H$_{47}$O$_9$N$_9$F$_2$Cl$_2$Fe$_2$: C, 43.15 (42.65); H, 5.01 (4.68); N, 13.32 (13.54), F, 4.01 (4.29).

2.2.2. [Fe$_2$(μ-O)(bpmen)$_2$(OOCCH$_3$)F](ClO$_4$)$_2$·2CH$_3$CN (4)

Tetrabutylammonium fluoride 75% in water (34 mg, 0.10 mmol) dissolved in 5 mL ethanol was added to a 15 mL acetonitrile solution of complex [Fe$_2$(μ-O)(μ-OOCCH$_3$)-(bpmen)$_2$](ClO$_4$)$_3$ (2). The mixture was stirred for several minutes and its color changed from brown to orange. Orange crystals suitable for X-ray diffraction analysis were obtained by vapor diffusion of diethyl ether into this solution. In situ ESI-MS(+)(CH$_3$CN): *m/z* 845 ({[Fe$_2$(μ-O)(OOCCH$_3$)-(F)(bpmen)$_2$](ClO$_4$)}$^+$, 8), 373 ({[Fe$_2$(μ-O))(OOCCH$_3$)(F)(bpmen)$_2$]}$^{2+}$, 18), 242 ({Bu$_4$N}$^+$, 100).

2.2.3. [Fe$_2$(μ-O)(bpmen)$_2$(OOCCH$_3$)$_2$](ClO$_4$)$_2$·2H$_2$O (5)

Red crystals suitable for X-ray diffraction analysis were obtained by vapor diffusion of diethyl ether into an acetonitrile solution of [Fe$_2$(μ-O)(μ-OH)(bpmen)$_2$](ClO$_4$)$_3$ (1) (2.0 mL, 2.0 μmol) in the presence of 1–3 molar equivalents of acetate, or after successive addition of acetate and acetic acid to 1. In situ ES-MS(+) (CH$_3$CN): *m/z* 925 ({[Fe$_2$(μ-O)(μ-OOCCH$_3$)-(bpmen)$_2$](ClO$_4$)}$^+$, 10), 885 ({[Fe$_2$(μ-O)(OOCCH$_3$)$_2$-(bpmen)$_2$](ClO$_4$)}$^+$, 14), 393 ({[Fe$_2$(μ-O))(OOCCH$_3$)$_2$-(bpmen)$_2$]}$^{2+}$, 52), 385 ({[Fe(OOCCH$_3$)(bpmen)]}$^+$, 92), 242 ({Bu$_4$N}$^+$, 100).

Complex 5 was also obtained by reacting [Fe$_2$(μ-O)(μ-OOCCH$_3$) (bpmen)$_2$](ClO$_4$)$_3$ (2) in acetonitrile (2.0 mL, 2.0 μmol) with equimolar amounts of acetate. In situ

ES-MS(+) (CH$_3$CN): *m/z* 885 ({[Fe$_2$(μ-O)(OOCCH$_3$)$_2$-(bpmen)$_2$](ClO$_4$)}$^+$, 70), 393 ({[Fe$_2$(μ-O)(OOCCH$_3$)$_2$(bpmen)$_2$]}$^{2+}$, 100), 385 ({[Fe(OOCCH$_3$)(bpmen)]}$^+$, 86), 242 ({Bu$_4$N}$^+$, 4).

2.3. X-ray diffraction studies

Pertinent crystallographic data and experimental conditions are summarized in Table 1.

Suitable crystals of 3–5 were mounted on a glass fiber using glue. Data were collected using a Bruker SMART CCD (charge coupled device) based diffractometer operating at 293–298 K. Data were measured using omega scans of 0.3° per frame for 30 s, such that a hemisphere was collected. A total of 1650 frames were collected with a maximum resolution of 0.75 Å. Cell parameters were retrieved using SMART [29,30] software and refined using SAINT [31,32] on all observed reflections. Data reduction was performed using the SAINT software which corrects for Lorentz and polarization effects. Absorption corrections were applied using SADABS [33] for complex 4. The structures of complexes 3 and 4 were solved by Patterson method and the structure of complex 5 was solved by the direct method using the SHELXS-90 [34] program and refined by least squares method on F^2, SHELXL-97 [35], incorporated in SHELXTL [36,37]. Hydrogen atoms were calculated by geometrical methods and refined as a riding model. For complexes 3 and 4, all non-hydrogen atoms were refined anisotropically. For complex 5, only the iron and chlorine atoms were refined anisotropically.

For complex 4, poor quality of the data set (low peak intensity with mean I/sigma ratio of 2.25) resulted in high *w*R2 factor after refinement. Although the precision on bond lengths and angles is affected by this problem, the nature and connectivity of all atoms in the structure could be determined with no ambiguity. Our attempts to obtain better quality crystals did not succeed.

Table 1
Crystallographic data for [Fe$_2$(μ-O)(BPMEN)$_2$F$_2$](ClO$_4$)$_2$·2(CH$_3$CN) (3), [Fe$_2$(μ-O)(BPMEN)$_2$(OOCCH$_3$)F](ClO$_4$)$_2$·2(CH$_3$CN) (4) and low-precision data for [Fe$_2$(μ-O)(BPMEN)$_2$(OOCCH$_3$)$_2$](ClO$_4$)$_2$·2(H$_2$O) (5)

	3·2(CH$_3$CN)	4·2(CH$_3$CN)	5·2(H$_2$O)
Empirical formula	C$_{36}$H$_{50}$Cl$_2$F$_2$Fe$_2$N$_{10}$O$_9$	C$_{38}$H$_{53}$Cl$_2$FFe$_2$N$_{10}$O$_{11}$	C$_{36}$H$_{47}$Cl$_2$Fe$_2$N$_8$O$_{15}$
Formula weight (amu)	987.46	1027.50	1018.45
Crystal habit, color	Needle, orange	Needle, orange	Plate, red
Crystal system	Triclinic	Triclinic	Triclinic
Space group	*P*-1	*P*-1	*P*-1
a (Å)	7.7016(14)	11.566(4)	13.0721(19)
b (Å)	11.452(2)	14.045(5)	13.305(2)
c (Å)	13.306(3)	16.115(5)	14.399(2)
α (°)	69.831(4)	100.863(7)	79.392(3)
β (°)	82.782(5)	109.693(9)	84.610(3)
γ (°)	81.907(4)	102.687(7)	75.985(3)
V (Å^3)	1086.8 (4)	2304.3(13)	2385.1(6)
Z	1	2	2
D_c (g. cm^{-3})	1.509	1.481	1.418
Crystal size (mm)	0.40 × 0.06 × 0.05	0.30 × 0.06 × 0.04	0.18 × 0.12 × 0.05
R1 [*I* > 2sigma(*I*)]	0.0978	0.1268	0.1488
*w*R2 [*I* > 2sigma(*I*)]	0.2575	0.3078	0.3974

The structure of complex **5** was found to be more problematic. Due to the data quality further refinement was unsuccessful. In our hands we could not find any twin, rotations or other possible factors to the poor data quality. Several data sets were tried, the best refined to R1 = 0.1474. The crystal used for the diffraction study showed no decomposition during data collection. Although these data only provides preliminary information on the crystal structure of complex **5**, the nature and connectivity of all atoms in the structure could be determined with no ambiguity.

2.4. Catalysis experiments

Solutions of iron(III) complexes were prepared by dissolving the corresponding precursor complex **1**, **2** or **3** (7.2 μmol, 5% catalyst) in 1.5 mL acetonitrile; various additives (i.e., hydrofluoric acid, tetrabutylammonium fluoride, acetic acid, or acetate) were added when necessary. Cyclooctene or 1-decene (0.3 mL, 0.144 mmol) premixed with nitrobenzene (internal standard, 0.058 mmol) was added to the catalyst solution. To this mixture, hydrogen peroxide from 30% stock solution in water (0.3 mL, 0.216 mmol) was added. 50 μL aliquots were taken before addition of hydrogen peroxide and after 5 min of reaction. These aliquots were immediately diluted in 1 mL of diethyl ether, filtered and analyzed by GC. Reaction yields and conversions reported are average of two runs. Final catalyst:substrate:H_2O_2 ratio = 1:20:30. Olefin epoxidations were typically run at room temperature.

2.5. Stopped-flow kinetic experiments

Rapid reactions between complex **1** and acetic acid or acetate were studied using a Hi-Tech Scientific (Salisbury, Wiltshire, UK) SF-43 cryogenic stopped-flow instrument with UV–vis spectrophotometric registration and a 1.00 cm mixing cell. The kinetic data from stopped-flow experiments were treated with the integral method, using the IS-2 Rapid Kinetics software by Hi-Tech Scientific. For the reaction with acetic acid, solutions of **1** (0.5 mM before mixing) and acetic acid (10–100 mM before mixing) were prepared at room temperature in acetonitrile. Kinetic measurements were performed at 25 °C by monitoring the disappearance of the 555 nm absorbance band characteristic of **1**. The kinetic curves at λ = 555 nm, obtained under pseudo-first-order conditions (complex **1** as limiting reagent), were fit to Eq. (1):

$$A_t = A_\infty - (A_\infty - A_0)\exp(-k_{obs}t) \qquad (1)$$

In all kinetic experiments, two to five shots gave standard deviations for k_{obs} below 6%.

For the reaction with acetate, stoichiometric conditions were used. Concentrations of **1** and acetate were 1 mM before mixing and temperatures were varied from −20 to 5 °C. The possibilities to vary experimental conditions were limited in this case: increasing the concentration of acetate resulted in precipitate formation, and increasing temperature increased reaction rate beyond the capabilities of the standard stopped-flow methodology.

3. Results and discussion

3.1. Ligand exchange studies

In this work, ligand exchange reactions at dinuclear iron(III)-bpmen complexes with hydrofluoric acid, fluoride, acetic acid and acetate as incoming ligands were performed for both $[Fe_2(III)(\mu\text{-}O)(\mu\text{-}OH)(bpmen)_2]^{3+}$ (**1**) and $[Fe_2(III)(\mu\text{-}O)(\mu\text{-}OAc)(bpmen)_2]^{3+}$ (**2**) (Scheme 1). The addition of acid (HF or HOAc) to complex **1** (or **1a**) facilitated ligand exchange, because protonation of an oxo- or hydroxo-ligand generated coordinated water molecules as leaving groups. The ligand exchange reactions in acetonitrile solutions were followed by UV–vis and products were characterized by in situ ESI-MS. In several cases, open-core species with two terminal ligands were isolated and characterized crystallographically.

3.1.1. Ligand exchange at a μ-oxo, μ-hydroxo diiron diamond core

Complex **1** reacted with all four additives studied (F⁻, HF, CH_3COO^-, CH_3COOH). Upon mixing **1** with 1 equivalent of hydrofluoric acid, fluoride, or acetate, the characteristic band of **1** at 555 nm disappeared and featureless UV–vis spectra, which correspond to open-core species [10], were obtained (Fig. 1 and S1–S2). The formulations of these species (Scheme 1) are based on in situ ESI-MS data and should be treated with care.

Upon successive reaction of **1** with HF (1 eq) followed by F⁻ (1 eq), further changes (albeit minor) in the visible spectrum were observed (Fig. S2), and the difluoride open core species **3** was detected as the only diiron species in solution by ESI-MS (peak at m/z 805 corresponding to {[Fe₂(μ-O)(bpmen)₂F₂](ClO₄)}⁺). The difluoride complex was also independently synthesized by self assembly from iron(III) salt,

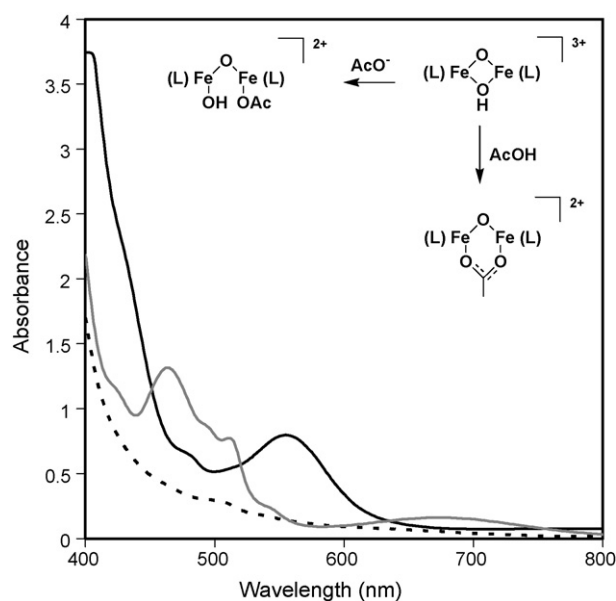
Fig. 1. Spectral changes upon reacting **1** ([**1**] = 1 mM) with 1 equivalent of acetate (- - -) or 1 equivalent of acetic acid (—) to form **2**. Absorbancies were adjusted for dilution.

bpmen, and two equivalents of fluoride in the presence of tri-ethylamine, and fully characterized. UV–vis and mass spectra for in situ generated **3** and for pure, independently prepared **3** were identical, and distinct from the spectra of the species formed in situ upon addition of 1 equivalent of F^- or HF to **1**.

Similarly, upon successive reaction of **1** with AcO$^-$ (1 eq) and AcOH (1 eq), the diacetate open core species **5** was detected as the only diiron species in solution by ESI-MS (peak at m/z 885 corresponding to $\{[Fe_2(\mu\text{-}O)(OOCCH_3)_2(bpmen)_2](ClO_4)\}^+)$. The diacetate complex was also independently prepared from **2** and acetate, and the spectra of this crystallographically characterized complex agree with the spectra of in situ prepared **5**. However, a direct reaction of **1** with acetic acid alone was previously known to yield a different product [12], the acetate-bridged dinuclear complex **2**. Our observations are in full agreement with this result: a characteristic visible spectrum of **2** confirms the formation of this complex upon mixing of acetonitrile solutions of **1** and acetic acid (Fig. 1).

In order to understand the effect of additives on the catalytic properties of Fe(III)-bpmen complexes, it was important to determine the time scale for ligand substitution at the diiron(III) core in complex **1**. Given that complex **1** yields different products upon reactions with acetate or with acetic acid, we were interested in comparing the relative rates of individual reaction steps in these two processes.

A stopped-flow study of the reaction of **1** with acetic acid showed that the characteristic band of **1** at 555 nm disappears with the concomitant appearance of the characteristic features of **2** (shown in Fig. 1). No open-core intermediates were observed. As was previously reported by Hazell et al. [12], the reaction takes several minutes, and time-resolved spectra show very tight isosbestic points. The reaction rates, however, were not characterized quantitatively in previous studies. We now performed concentration dependence experiments at 25 °C under pseudo-first order conditions (see experimental section). All reactions followed a single exponential change of optical absorbance indicating a process that was first order in complex **1**. Identical values of the observed rate constants were obtained at different wavelengths, confirming that the rate of decay of **1** is equal to the rate of formation of **2**. The plot of the observed rate constant versus acetic acid concentration is a straight line with nonzero intercept (Fig. 2), showing that the rate limiting step is a reversible bimolecular reaction with a second-order rate constant $k_1 = 1.6\,\text{M}^{-1}\,\text{s}^{-1}$ (determined as a slope of the straight line in Fig. 2) and an equilibrium constant $K = k_1/k_{-1} = 150 \pm 10\,\text{L}\,\text{mol}^{-1}$ at 25 °C (where k_{-1} is the intercept of the straight line in Fig. 2).
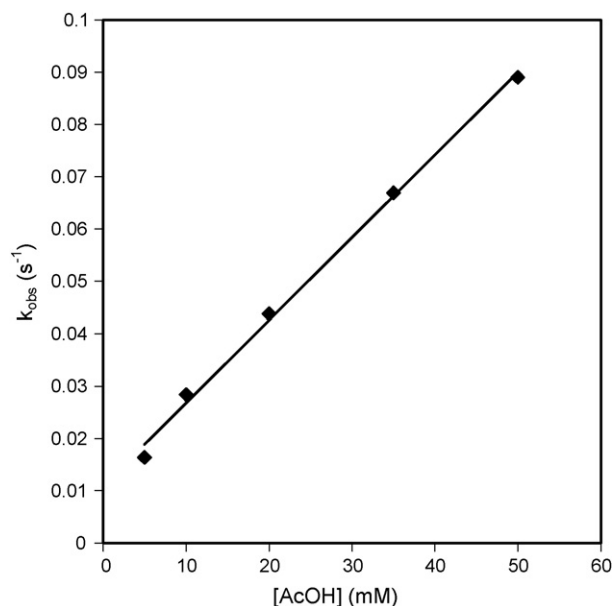

Fig. 2. Plot of the observed rate constant at 555 nm versus acetic acid concentration, after mixing with **1**, acquired by stopped-flow technique at 25 °C (0.25 mM of **1** and 5–50 mM of acetic acid after mixing).

We previously observed a stepwise reaction of **1** with bidentate ligands, such as urea [10]. Unlike the reaction between **1** and urea [10], where two distinct observable steps were identified, only one step was observed with acetic acid, although the structures of the final products are very similar in both cases. It is reasonable to assume that the general mechanism of the reaction between **1** and acetic acid also includes two steps: initial coordination of the ligand to one of the iron(III) centers, followed by an essentially irreversible ring closure step (Scheme 2). The k_1 for the reaction between **1** and acetic acid ($1.6\,\text{M}^{-1}\,\text{s}^{-1}$) is very similar to the rate constants of the first steps of the reactions of **1** with water ($k_1 = 1.6\,\text{M}^{-1}\,\text{s}^{-1}$), and substituted ureas and urea derivatives (k_1 ranges from 1.5 to $6.7\,\text{M}^{-1}\,\text{s}^{-1}$) [10]. It thus appears that the rate constant of the observed reaction step in the interaction between **1** and acetic acid corresponds to the process of initial coordination of an oxygen of H(OAc) to one iron(III) center, accompanied by a release of one water molecule. The following events (a proton transfer from coordinated HOAc to the hydroxide group and nucleophilic attack of the water molecule at the second iron center by the coordinated acetate) are expected to be rapid.

The direct reaction between **1** and acetate proved to be very rapid: it is complete in seconds at low temperatures (from −20 to +5 °C). Although detailed kinetic study was impossible for
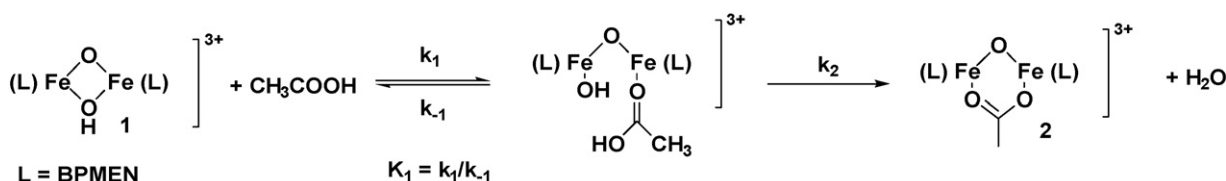
Scheme 2. Proposed sequence of reaction steps for the formation of **2** from **1** and acetic acid.

this reaction, which was complicated by precipitate formation in the presence of excess acetate, extrapolation or the observed rate constants to room temperature using the activation energy $E_a = 17$ kcal/mol (Fig. S3) conclusively demonstrated that **1** reacts with OAc⁻ 2–3 orders of magnitude faster than it reacts with acetic acid. This finding is in a good agreement with the higher nucleophilic character of OAc⁻, which is expected to facilitate otherwise similar ligand substitution reactions. Reactions of **1** with other anions are also expected to be similarly rapid.

3.1.2. Ligand exchange at a μ-oxo, μ-acetato ring closed diiron core

While complex **1** was previously known to undergo ligand substitution at its core, no study of ligand substitution at the μ-oxo, μ-acetate core of complex **2** has been reported as of now. This complex however has been controversially proposed to be catalytically active in epoxidation reactions [17,18,28]. Such catalytic properties could be due to a 'carboxylate shift' occuring at the diiron core, thus liberating a coordination site available for catalysis [17]. The reaction products of complex **2** with fluoride and acetate were determined in this study.

Upon mixing $[Fe_2(III)(\mu\text{-}O)(\mu\text{-}OAc)(bpmen)_2]^{3+}$ (**2**) with Bu_4NF, the characteristic spectral features of complex **2** disappear (Fig. 3). The acetate-bridged core opens up to form $[Fe_2(\mu\text{-}O)(bpmen)_2(OAc)F](ClO_4)_2$ (**4**), which has been detected in solution by ESI-MS. The spectral changes observed indicate an essentially irreversible process with a linear decrease in absorbance with an increase in fluoride concentration, which occurs until 1 molar equivalent of fluoride was added. Addition of excess of fluoride did not affect the final spectrum of **4** (Fig. 3). In agreement with observed stoichiometry in solution, a mixed-ligand acetate-fluoride complex was isolated, and
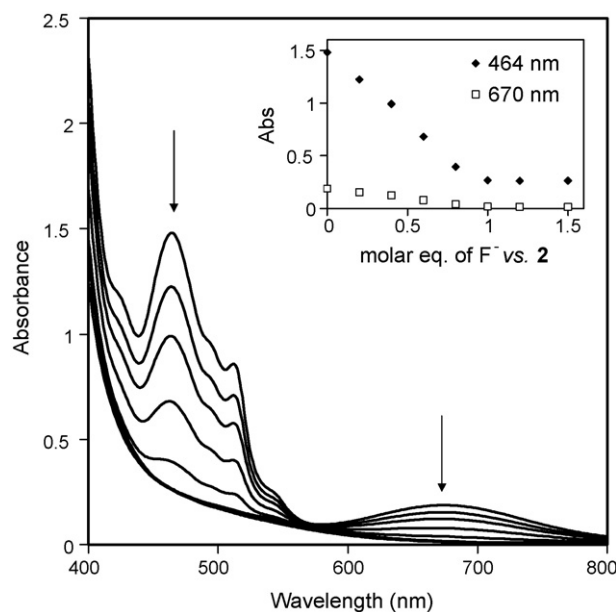

Fig. 3. Spectral changes upon addition of different amounts of fluoride to **2** to form **4** ([**2**] = 1 mM, 0–1.5 molar equivalents of F⁻ added). Absorbancies were adjusted for dilution. Inset shows the cross sections at 464 nm and 670 nm.

crystallographically characterized. UV–vis spectra of the crystallographically characterized **4** are identical to the spectra of this complex generated in situ.

Complex **2** did not react with equivalent amounts of protonated ligands (either HF or acetic acid). Adding excess (10 equivalents) of HOAc did not give rise to any spectral changes, while adding 10 equivalents of HF resulted in very minor spectral changes. In contrast, complex **2** reacted with acetate to form the diacetate complex $[Fe_2(\mu\text{-}O)(bpmen)_2(OOCCH_3)_2](ClO_4)_2$ (**5**), detected by UV–vis and ESI-MS (Fig. S4). The carboxylate bridge in complex **2** can therefore be displaced by nonprotonated coordinating anions like F⁻ or acetate but not by their corresponding neutral acid forms.

3.2. Isolation and structural characterization of complexes 3–5

Three open-core diiron(III) complexes bearing additional ligands at each iron(III) center were isolated in the solid state, and X-ray quality crystals were obtained. Complex $[Fe_2(\mu\text{-}O)(bpmen)_2F_2](ClO_4)_2$ (**3**) bearing two fluorides was prepared by sequential addition of HF and F⁻ to **1**, and was also independently prepared by self assembly from iron(III) salt, bpmen, and two equivalents of fluoride in the presence of triethylamine. Complex $[Fe_2(\mu\text{-}O)(bpmen)_2(OOCCH_3)F](ClO_4)_2$ (**4**) featuring an unusual asymmetric core with one fluoride and one acetate on each iron was prepared by reacting **2** with an equimolar amount of fluoride. Complex $Fe_2(\mu\text{-}O)(bpmen)_2(OOCCH_3)_2](ClO_4)_2$ (**5**) bearing two acetates was prepared by sequential addition of AcO⁻ and AcOH to **1** or by reacting **2** with equimolar amount of acetate (Scheme 1).

Complexes **3** and **4** were structurally characterized (Fig. 4). A low precision crystal structure was also obtained for complex **5** showing the nature and connectivity of all atoms in the complex with no ambiguity (Fig. 5). These compounds are structurally similar to each other and consist of two $Fe^{III}(bpmen)$ moieties bridged by an oxo group and each iron center bearing a terminal ligand (fluoride or acetate) (Figs. 4 and 5). In all cases, the *cis*-α conformation of bpmen is similar to the previously characterized diiron(III) complexes of this ligand [10–15] and the Fe-N bond lengths (2.14–2.28 Å) in **3** and **4** are in the typical range for high-spin iron(III) complexes (Table 2).

The solid-state structure of complex **3**, with only half a molecule found per asymmetric unit, revealed that the bridging oxygen lies on a center of symmetry thus indicating a 180° Fe–O–Fe angle. For the asymmetric fluoride/acetate complex **4**, an angle of 172° was found (Table 2). For both complexes, the monodentate ligands are *trans* with respect to the Fe–O–Fe moiety (torsional angles X–Fe–Fe–X are 180° for **3**, 172° for **4**). This geometry is different from the *cis*-orientation of water and hydroxo ligands in $[(bpmen)(H_2O)Fe(\mu\text{-}O)Fe(OH)(bpmen)]^{3+}$, which allows for a strong intramolecular hydrogen bonding between the two terminal ligands [14]. The orientation of chloride ligands in two different solvates of $[(bpmen)(Cl)Fe(\mu\text{-}O)Fe(Cl)(bpmen)]^{2+}$ is generally similar to the *trans*-geometry of **3**, although substantial deviations from the ideal Cl–Fe–Fe–Cl torsional angle of 180° were found (torsional angles of 128.2°
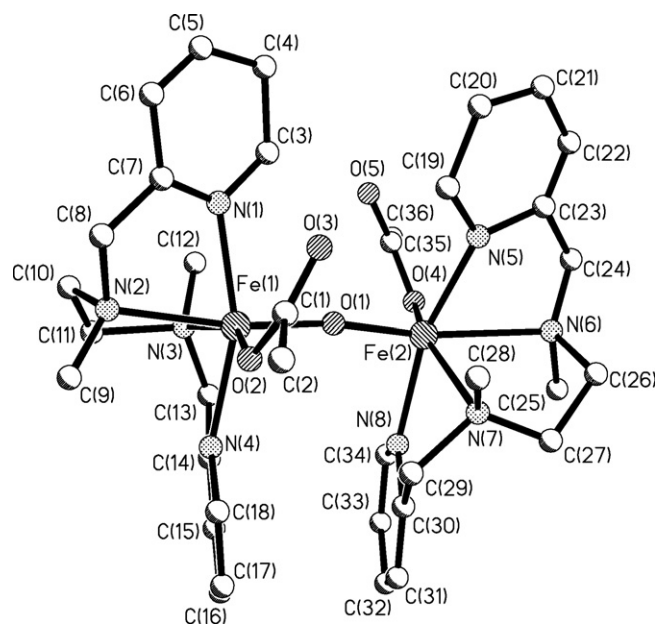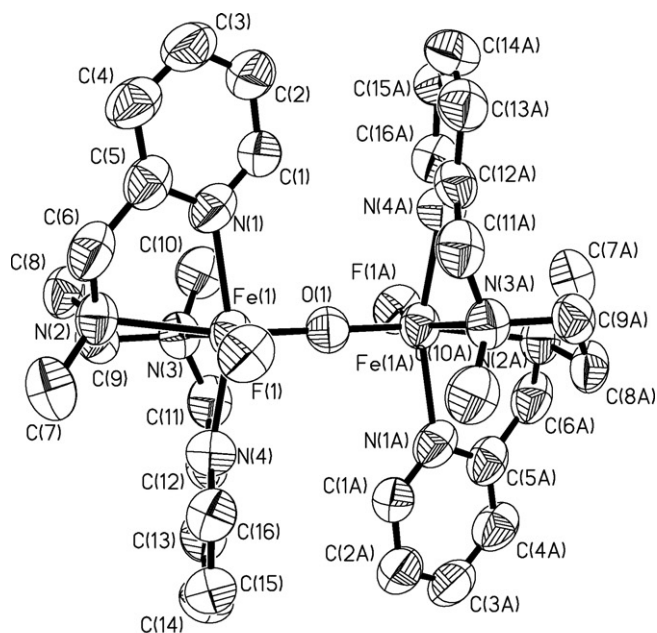
Fig. 4. Representation of the X-ray structure of the complex cation in **3** (top) and **4** (bottom), showing 50% probability thermal ellipsoids. Hydrogen atoms are not included for clarity.

Fig. 5. Representation of the X-ray structure of the complex cation in **5**. Hydrogen atoms are not included for clarity.

trans or pseudo-*trans* geometry with respect to the Fe–O–Fe moiety. This arrangement is very different from the related diacetate diiron(II) complex of bpmen previously characterized where the two acetate group were found bridging the iron atoms in the absence of any oxo bridge [12].

3.3. Catalytic olefin epoxidation

The reactivity of iron complexes with bpmen in epoxidation of cyclooctene and 1-decene using hydrogen peroxide as the oxidant was tested, and the results are summarized in Tables 3 and 4. The high catalytic activity of the mononuclear iron(II) complex, [Fe(bmpen)(CH$_3$CN)$_2$]$^{2+}$, previously reported

Table 2
Selected bond lengths (Å) and angles (°) for [Fe$_2$(μ-O)(BPMEN)$_2$-F$_2$] (ClO$_4$)$_2$·2(CH$_3$CN) (**3**) and [Fe$_2$(μ-O)(BPMEN)$_2$(OOCCH$_3$)F](ClO$_4$)$_2$·2(CH$_3$CN) (**4**)

	3·2(CH$_3$CN)	4·2(CH$_3$CN)
Fe–O	1.8012(9)	1.821(6) (Fe1)
	–	1.788(6) (Fe2)
Fe–X	1.843(3)	1.912(8) (O2)
	–	1.861(6) (F1)
Fe–N(L)	2.235(5) (N3)	2.204(8) (N3)
In-plane	2.305(5) (N2)	2.279(9) (N2)
	–	2.229(9) (N6)
	–	2.277(9) (N7)
Fe–N(L)	2.135(6) (N4)	2.140(8) (N1)
Out-of-plane	2.179(6) (N1)	2.146(8) (N4)
	–	2.143(8) (N8)
	–	2.156(8) (N5)
Fe–O–Fe	180.000(1)	172.4(4)

X = F, O(Ac).

and 135° were found for iron(III)-bpmen dichloride complexes [15,38], and an angle of 140° was observed in a related dichloride complex supported by *N*-methyl-*N*-picolyl derivative of the bpmen ligand [39]). It follows that the Fe–O–Fe unit supported by two bpmen ligands is relatively flexible, and accommodates various orientations of terminal monodentate ligands. The electronic properties of Cl$^-$ terminal ligands are similar to those of F$^-$ ligands, and the somewhat different orientations of these ligands are probably due to steric effects.

The preliminary solid-state structure of complex **5** revealed two monodentate acetate each bound to one iron center also in a

Table 3
Epoxidation of cyclooctene with H_2O_2 catalyzed by iron complexes with bpmen

Additives	Temperature (°C)	Epoxide yield (%)	Diol yield (%)	Conversion (%)	Reference
$Fe_2(III)(\mu-O)(\mu-OH)$ (bpmen)$_2$(ClO$_4$)$_3$ (**1**)					
–	r.t.	39	5	61	This work
1 HF	r.t.	39	5	61	This work
1 F$^-$	r.t.	3	3	18	This work
1 AcOH	r.t.	25	4	46	This work
10 AcOH	r.t.	<0.1	<0.1	4	This work
1 AcO$^-$	r.t.	3	4	20	This work
$Fe_2(III)(\mu-O)(\mu-OAc)$(bpmen)$_2$(ClO$_4$)$_3$ (**2**)					
–	r.t.	<0.1	<0.1	5	This work
1 HF	r.t.	<0.1	<0.1	6	This work
1 F$^-$ (major species in solution: complex **4**)	r.t.	1	1	11	This work
1 AcOH	r.t.	<0.1	<0.1	5	This work
1 AcO$^-$ (major species in solution: complex **5**)	r.t.	2	2	12	This work
$Fe_2(III)(\mu-O)(F)_2$(bpmen)$_2$(ClO$_4$)$_2$ (**3**)					
–	r.t.	<0.1	<0.1	4	This work
Fe(II)(bpmen)(CH$_3$CN)$_2$(OTf)$_2$[a]					
–	r.t.	89.7	4.8	94	Ref. [19] [a]
34 AcOH	r.t.	102	2.7	105	Ref. [19] [a]
Fe(II)(bpmen)(CH$_3$CN)$_2$(SbF$_6$)$_2$					
10 AcOH	4	86 (isolated yield)	–	–	Ref. [17]
Fe(II)(bpmen)(CH$_3$CN)$_2$(ClO$_4$)$_2$[a]					
–	30	75	9		Ref. [16] [a]

Reactions were run in acetonitrile for 5 min; final catalyst:substrate:H_2O_2 ratio = 1:20:30.

[a] Iron complex was used as a limiting reagent; hydrogen peroxide was gradually added, over 5 min, via syringe pump.

by Que and coworkers [16,18,19] and Jacobsen and coworkers [17] (Tables 3 and 4), was reproduced in our experiments (Table 4), thus confirming the reliability of our experimental methodology. In agreement with published data [17,19], the effect of non-coordinating anions on the epoxide yields was relatively minor (in our repetitive experiments, the differences in catalytic activity of the perchlorate, triflate, and hexafluoroantimonate salts of Fe(bpmen)$^{2+}$ were comparable to the statistical variations in a series of independent catalytic runs with the same counterion), while addition of 1–10 equivalents of acetic acid with respect to Fe(bpmen)$^{2+}$ invariably improved the efficiency and selectivity of epoxide formation. In contrast, additions of HCl and, especially, HF decreased epoxide yields (Table 4).

The catalytic activity in olefin epoxidation of all dinuclear iron(III) complexes characterized in this work was also tested. The data for cyclooctene epoxidation, reported in Table 3, are summarized below. Complex **1**, which can easily undergo ring opening in the presence of water [10,14], was found to be catalytically active. Yields of 39% in epoxide with high selectivity (89%) with respect to the formation of diol were obtained after 5 min of reaction at room temperature and a 5% iron complex load. The overall selectivity is not great, however, as follows from the olefin consumption that significantly exceeds combined yield of the epoxide and the diol (Table 3), and is much lower than the selectivity in Fe(II)(bpmen)-catalyzed reactions [16–19]. Other oxidation products were not identified. While it may be possible to optimize the reaction conditions for the diiron(III) catalyst **1** and improve the epoxide yields, the emphasis of the present work is to compare the reactivity of monoiron(II) and diiron(III) complexes under otherwise identical conditions.

Addition of 1 equivalent of hydrofluoric acid to the solution of **1** did not affect the epoxidation of cyclooctene. The predominant iron-containing species in solution under these conditions is an open-core monofluoride [Fe$_2$(μ-O)(bpmen)$_2$F(OH$_2$)](ClO$_4$)$_2$ detected by ESI-MS and UV–vis (Section 3.1.1). In contrast, addition of fluoride or acetate (resulting in the formation of [Fe$_2$(μ-O)(bpmen)$_2$(F)(OH)](ClO$_4$) or [Fe$_2$(μ-O)(bpmen)$_2$(OAc)(OH)](ClO$_4$) complexes in solution, respectively, as suggested by UV–vis data shown in Fig. 1 and S1) inhibited the catalyst. The addition of stoichiometric amounts of acetic acid lowered the epoxide yields to 25% and total inhibition was observed in the presence of excess of acetic acid, where an acetate-bridged core complex **2** is formed. The time scale for the formation of **2** from **1** and HOAc (several minutes, as determined in kinetic experiments) is comparable to the epoxidation time (5 min) used in this work and in previously published reports [17–19,28]. Best catalysis results with **1** were therefore obtained when a labile site at one of the iron centers is present (Table 3). The coordination of more strongly bound ligands, like monodentate hydroxide, fluoride or acetate provided as additives, to both iron(III) centers resulted in much lower activity (Table 3).

Complexes **2** and **3** did not promote any cyclooctene epoxidation under our reaction conditions. The presence of additives (Table 3) did not affect the reactivity of **2** as a catalyst. The 'carboxylate shift' observed when **2** is mixed with non-protonated fluoride or acetate, yielding complexes **4** or **5**, did not increase

Table 4
Epoxidation of decene with H_2O_2 catalyzed by iron complexes with bpmen

Additives	Temperature (°C)	Epoxide yield (%)	Reference
$Fe_2(III)(\mu\text{-}O)(\mu\text{-}OH)$ (bpmen)$_2$(ClO$_4$)$_3$ (**1**)			
–	4	7	This work
–	40	20	This work
10 AcOH	4	4	This work
10 AcOH	40	6	This work
$Fe_2(III)(\mu\text{-}O)(\mu\text{-}OAc)$(bpmen)$_2$(ClO$_4$)$_3$ (**2**)			
–	4	0	This work
–	4	2 (oct-1-ene)	Ref. [18]
–	4	82	Ref. [17]
–	40	1	This work
10 AcOH	4	1	This work
10 AcOH	40	1	This work
$Fe_2(III)(\mu\text{-}O)(F)_2$(bpmen)$_2$(ClO$_4$)$_2$ (**3**)			
–	4	0	This work
–	40	<1	This work
10 AcOH	40	<1	This work
$Fe(II)$(bpmen)(CH$_3$CN)$_2$(ClO$_4$)$_2$			
–	4	40	Ref. [17]
–	4	82	This work
1 HCl	4	50.5 (conversion: 69.8%)	This work
1 HF	4	21.2 (conversion:38.8%)	This work
1 AcOH	4	> 99	This work
10 AcOH	4	>99	This work
$Fe(II)$(bpmen)(CH$_3$CN)$_2$(OTf)$_2$			
-	0	49	Ref. [19]
10 AcOH	0	63	Ref. [19]
$Fe(II)$(bpmen)(CH$_3$CN)$_2$(SbF$_6$)$_2$			
–	4	63	This work
–	4	71	Ref. [17]
–	4	73 (oct-1-ene)	Ref. [18]
–	0	70	Ref. [19]
10 AcOH	4	>99	This work
10 AcOH	4	85	Ref. [17]
10 AcOH	0	82	Ref. [19]

Reactions were run in acetonitrile for 5 min; final catalyst:substrate:H_2O_2 ratio = 1:20:30.

the epoxide yields, but higher conversions of alkene and traces of oxidized products were detected.

Catalytic epoxidation of 1-decene was also attempted. The results are generally similar to those described for epoxidation of cyclooctene, although the product yields were significantly lower for 1-decene. The data are summarized in Table 4.

3.4. Discussion

μ-Oxo diiron(III) complexes of aminopyridine ligands have been reported to catalyze a variety of oxidation reactions [2]. In particular, efficient catalysts for alkane hydroxylation are μ-oxo diiron(III) complexes of bipy (=2,2'-bipyridine) [40,41], tpa (=tris(2-pyridylmethyl)amine) [42] and tmima (tris[(1-methylimidazol-2-yl)methyl]amine) [43] with μ-acetate(s) and/or aqua ligands. The presence of bridging acetate usually resulted in lower reactivity under comparable conditions [40,41] whereas the presence of coordinated chlorides inhibited the catalysis.

More recently, μ-oxo diiron(III) complexes were also reported to catalyze alkene epoxidation [19,28,44,45]. Complex $[((phen)_2(H_2O)Fe^{III})_2(\mu\text{-}O)](ClO_4)_4$ (with phen = 1,10-phenanthroline) is a very efficient catalyst: epoxide formation is quantitative with peracetic acid as the oxidant [28]. However, the carboxylate bridged analogue $[((phen)_2Fe^{III})_2(\mu\text{-}O)(\mu\text{-}OAc)](ClO_4)_3$ and the chloride-containing analogue $[((phen)_2(Cl)Fe^{III})_2(\mu\text{-}O)](Cl)_2$ were found to be less active or inactive as terminal alkene epoxidation catalyst [28]. When hydrogen peroxide was used as the oxidant, much lower yields (13% at room temperature) were observed [19]. Addition of acetic acid further lowered the epoxide yield (down to 8% with 29 equivalents of acid) [19].

Lower cyclooctene epoxidation yields (5.7 TON in acetonitrile, which corresponds to 16% yield under the reaction conditions reported) were observed after 3 h when complex $[((mebpa)_2(Cl)Fe^{III})_2(\mu\text{-}O)](ClO_4)_2$ (with mebpa = N-(2-methoxyethyl)-N,N-bis(pyridine-2-yl-methyl)amine) is used with hydrogen peroxide as the oxidant [45]. In that case, addition of 10 equivalents of acetic acid did not significantly affect the catalysis (8.3 TON or 24% epoxide yield in presence of 10 eq AcOH) and spectroscopic properties of the reaction mixture. However, the addition of 2-pyrazinecarboxylic acid, which clearly reacts with $[((mebpa)_2(Cl)Fe^{III})_2(\mu\text{-}O)](ClO_4)_2$ as evidenced by the changes in the UV–vis spectra, resulted in a dramatic decrease in catalytic activity.

With complexes of bpmen, conflicting observations were reported on the reactivity of the μ-oxo, μ-acetate core of complex **2**. The first report indicating high catalytic activity of **2** focused on the bridged acetate complex formed *in situ* from Fe(II)(bpmen)(SbF$_6$)$_2$, glacial acetic acid, and H_2O_2 [17]. These solutions contained **2** according to a characteristic UV–vis spectrum, and were able to catalyze epoxidation of 1-decene upon further dropwise additions of H_2O_2 [17]. In our case, complex **2** also formed in the presence of H(OAc) under epoxidation conditions. Kinetic experiments suggest that the rate of ring closure with acetic acid is at least comparable to (and usually much higher than) the reaction times used in typical epoxidation experiments. However, independently prepared pure complex **2** did not catalyze the epoxidation of cyclooctene or 1-decene under comparable conditions whereas complex **1** did (Tables 3 and 4), thus confirming another report stating the inactivity of **2** in olefin epoxidation of terminal olefins [18].

In our hands, coordinated fluorides and/or terminal acetates also inhibited the catalytic activity of **1**. Furthermore, independently prepared complex **3** and generated in situ complexes **4** and **5** were also catalytically inactive. These results are in accord with previous findings on catalysis inhibition upon mono- or bidentate ligand coordination to diiron cores, which were discussed above.

The diiron(III) complex **1,** which can easily open to form complex **1a** with a labile aqua ligand at one of the iron centers, acts as a catalyst of alkene epoxidation with H_2O_2 (Tables 3 and 4). The finding of moderate catalytic activity and good selectivity in cyclooctene epoxidation displayed by diiron(III) complex **1** (8 turnovers were observed under our experimental conditions) is promising for the design of air-

stable epoxidation catalysts. However, the catalytic activity of this complex does not match the very high catalytic efficiency and selectivity of its mononuclear iron(II) counterpart, $[Fe(bpmen)(CH_3CN)_2]^{2+}$. The relatively low catalytic activity of dinuclear iron(III)-bpmen complexes, measured under the same conditions as the high activity of the mononuclear iron(II) complex $[Fe(bpmen)(CH_3CN)_2]^{2+}$, argues against the involvement of a dinuclear intermediate in the course of olefin epoxidation with $H_2O_2/[Fe(bpmen)(CH_3CN)_2]^{2+}$. These complexes also display different responses to additives (especially HOAc, Tables 3 and 4). The μ-oxo-μ-acetato-bridged complex **2**, which was proposed as an active intermediate in epoxidations with $H_2O_2/[Fe(bpmen)(CH_3CN)_2]^{2+}$/HOAc [17], lacks catalytic activity and cannot be responsible for the highly efficient and selective epoxide formation (Tables 3 and 4).

We propose, by analogy with published data for related aminopyridine diiron(III) complexes [26,46], that a likely intermediate in the diiron(III) system containing complex **1** and H_2O_2 is a hydroperoxo species, which may react non-selectively, and generate various active oxidants (including, perhaps, hydroxyl radicals). Unfortunately, peroxo-intermediates in iron–bpmen systems proved to be unstable, and were only observed, in low yield, below −60 °C by EPR spectroscopy [47]. While our present data do not allow us to unambiguously exclude dissociation of the dinuclear complex **1** into catalytically active monomeric subunits under epoxidation conditions, a report on the diiron(III) complex with a dinucleating, covalently linked tris-picolylamine (TPA) derivative confirms high reactivity in olefin epoxidation of oxo-bridged diiron(III) species bearing terminal water ligands [26]. In the latter case, the diiron-peroxo intermediate was observed, and the oxidation products were different from those obtained with a related mononucleating, monomeric catalyst (predominantly epoxides were formed with the diiron(III) catalyst [26], and predominantly diols were obtained with a monoiron(II)-TPA catalyst [16,18,19]). Further mechanistic investigations on diiron(III) reactivity with hydrogen peroxide and peroxo-acids (which account for higher epoxide yields in related systems [19,28] in bpmen-supported complexes are in progress.

4. Conclusions

Ligand substitution reactions at doubly bridged μ-oxo, μ-hydroxo or μ-oxo, μ-acetato diiron(III) cores with fluoride and acetate as incoming ligands are reported. Complex $[Fe_2(\mu\text{-}O)(\mu\text{-}OH)(bpmen)_2](ClO_4)_3$ (**1**) reacted with both protonated and non-protonated ligands, whereas complex $Fe_2(III)(\mu\text{-}O)(\mu\text{-}OAc)(bpmen)_2$ (**2**) reacted exclusively with the non-protonated, anionic forms, yielding three novel diiron(III) complexes which were structurally characterized. The crystalline complexes, $[Fe_2(\mu\text{-}O)(bpmen)_2F_2](ClO_4)_2$ (**3**) bearing two fluorides and $[Fe_2(\mu\text{-}O)(bpmen)_2(OOCCH_3)F](ClO_4)_2$ (**4**) featuring an unusual asymmetric core with one fluoride and one acetate on each iron, adopted trans-orientation of monodentate ligands with respect to nearly linear Fe–O–Fe fragment. Comparative catalysis experiments showed that diiron(III) complex **1** can catalyze the epoxidation of cyclooctene with hydrogen peroxide at room

temperature. While addition of HF did not affect the catalysis, other additives (especially F^- and OAc^-) inhibited the reactivity of **1**. Complexes **2–5** did not catalyze this reaction thus confirming that the presence of a labile site at one of the iron centers is necessary.

Appendix A. Supplementary data

Supplementary data associated with this article can be found, in the online version, at doi:10.1016/j.molcata.2006.05.071.

References

[1] D.M. Kurtz Jr., Chem. Rev. 90 (1990) 585–606.
[2] M. Fontecave, S. Ménage, C. Duboc-Toia, Coord. Chem. Rev. 180 (1998) 1555–1572.
[3] E.Y. Tshuva, S.J. Lippard, Chem. Rev. 104 (2004) 987–1012.
[4] P. Nordlund, H. Eklund, Curr. Opin. Struct. Biol. 5 (1995) 758–766.
[5] D.E. Wilkox, Chem. Rev. 96 (1996) 2435–2458.
[6] D.M. Kurtz Jr., J. Biol. Inorg. Chem. 2 (1997) 159–167.
[7] E.I. Solomon, T.C. Brunold, M.I. Davis, J.N. Kemsley, S.K. Lee, N. Lehnert, F. Neese, A.J. Skulan, Y.S. Yang, J. Zhou, Chem. Commun. (2000) 235–349.
[8] K. Chen, L. Que Jr., Chem. Commun. (1999) 1375–1376.
[9] P. Mialane, L. Tchertanov, F. Banse, J. Sainton, J.J. Girerd, Inorg. Chem. 39 (2000) 2440–2444.
[10] S. Taktak, S.V. Kryatov, E.V. Rybak-Akimova, Inorg. Chem. 43 (2004) 7196–7209.
[11] N. Arulsamy, P.A. Goodson, D.J. Hodgson, Inorg. Chim. Acta 216 (1994) 21–29.
[12] R. Hazell, K.B. Jensen, C.J. McKenzie, H. Toflund, J. Chem. Soc. Dalton Trans. (1995) 707–717.
[13] T. Okuno, S. Ito, S. Ohba, Y. Nishida, Dalton Trans. (1997) 3547–3551.
[14] S. Poussereau, G. Blondin, M. Cesario, J. Guilhem, G. Chottard, F. Gonnet, J.-J. Girerd, Inorg. Chem. 37 (1998) 3127–3132.
[15] R.K. Egdal, R. Hazell, C.J. McKenzie, Acta Cryst. C E58 (2002) m10–m12.
[16] M. Costas, A.K. Tipton, K. Chen, D.-H. Jo, L. Que Jr., J. Am. Chem. Soc. 123 (2001) 6722–6723.
[17] M.C. White, A.G. Doyle, E.N. Jacobsen, J. Am. Chem. Soc. 123 (2001) 7194–7195.
[18] J.Y. Ryu, J. Kim, M. Costas, K. Chen, W. Nam, L. Que Jr., Chem Commun. (2002) 1288–1289.
[19] M. Fujita, L. Que Jr., Adv. Synth. Catal. 346 (2004) 190–194.
[20] S. Taktak, M. Flook, B.M. Foxman, L. Que Jr., E.V. Rybak-Akimova, Chem. Commun. (2005) 5301–5303.
[21] K. Chen, M. Costas, J. Kim, A.K. Tipton, L. Que Jr., J. Am. Chem. Soc. 124 (2002) 3026–3035.
[22] K. Chen, M. Costas, L. Que Jr., Dalton Trans. (2002) 672–679.

[23] M.V. Twigg, J. Burgess, in: J.A. McCleverty, T.J. Meyer (Eds.), Comprehensive Coordination Chemistry II, vol. 5, Elsevier, Oxford, 2004, pp. 403–553.

[24] S.J. Lange, H. Miyake, L. Que Jr., J. Am. Chem. Soc. 121 (1999) 6330–6331.

[25] M.P. Jensen, S.J. Lange, M.P. Mehn, E.L. Que, L. Que Jr., J. Am. Chem. Soc. 125 (2003) 2113–2128.

[26] M. Kodera, M. Itoh, K. Kano, T. Funabiki, M. Reglier, Angew. Chem. Int. Ed. 44 (2005) 7104–7106.

[27] H. Zheng, Y. Zang, Y. Dong, V.G. Young Jr., L. Que Jr., J. Am. Chem. Soc. 121 (1999) 2226–2235.

[28] G. Dubois, A. Murphy, T.D.P. Stack, Org. Lett. 5 (2003) 2469–2472.

[29] SMART V 5.054 (NT), S.V. Software for the CCD Detector System, Bruker Analytical X-ray Systems, Madisson, WI, 1998.

[30] SMART V 5, N. Software for the CCD Detector System, Bruker Analytical X-ray Systems, Madison, WI, 2001.

[31] SAINT V 6, N. Software for the CCD Detector System, Bruker Analytical X-ray Systems, Madison, WI, 1999.

[32] SAINT V 6, N. Software for the CCD Detector System, Bruker Analytical X-ray Systems, Madison, WI, 2001.

[33] R.H. Blessing, SADABS. Program for absorption corrections using Siemens CCD based on the method of Robert Blessing, Acta Crystallogr. A 51 (1995) 33–38.

[34] G.M. Sheldrick, SHELXS-90. Program for the Solution of Crystal Structure, University of Gottingen, Germany, 1990.

[35] G.M. Sheldrick, SHELXS-97. Program for the Refinement of Crystal Structure, University of Gottingen, Germany, 1997.

[36] SHELXTL 5.1, (PC-Version). Program library for Structure Solution and Molecular Graphics, Bruker Analytical X-ray Systems, Madison, WI, 1998.

[37] SHELXTL 6.1, (PC-Version). Program library for Structure Solution and Molecular Graphics, Bruker Analytical X-ray Systems, Madison, WI, 2000.

[38] N. Raffard, V. Balland, J. Simaan, S. Letard, M. Nierlich, K. Miki, F. Banse, E. Anxolabehere-Mallart, J.-J. Girerd, Comptes Rendus Chimie 5 (2002) 99–109.

[39] A.L. Nivorozhkin, E. Anxolabehere-Mallart, P. Mialane, R. Davydov, J. Guilhem, M. Cesario, J.-P. Audihre, J.-J. Girerd, S. Styring, L. Schussler, J.-L. Seris, Inorg. Chem. 36 (1997) 846–853.

[40] S. Ménage, J.M. Vincent, C. Lambeaux, M. Fontecave, J. Mol. Catal. A 113 (1996) 61–75.

[41] S. Ménage, J.M. Vincent, C. Lambeaux, G. Chottard, A. Grand, M. Fontecave, Inorg. Chem. 32 (1993) 4766–4773.

[42] J.H. Kim, C. Kim, R.G. Harrison, E.C. Wilkinson, L. Que Jr., J. Mol. Catal. A 117 (1997) 83–89.

[43] R.M. Buchanan, S. Chen, J.F. Richardson, M. Bressan, L. Forti, A. Morvillo, R.H. Fish, Inorg. Chem. 33 (1994) 3208–3209.

[44] X.M. Wang, S.X. Wang, L.J. Li, E.B. Sundberg, G.P. Gacho, Inorg. Chem. 42 (2003) 7799–7808.

[45] S. Tanase, C. Foltz, R. de Gelder, R. Hage, E. Bouwman, J. Reedijk, J. Mol. Catal. A 225 (2005) 161–167.

[46] S.V. Kryatov, E.V. Rybak-Akimova, J. Chem. Dalton Trans. (1999) 3335–3336.

[47] E.A. Duban, K.P. Bryliakov, E.P. Talsi, Mendeleev Commun. (2005) 12–14.